AN ACA ACCELERATED ISOGEOMETRIC BOUNDARY ELEMENT ANALYSIS

Lucas Silveira Campos

zaz1588@gmail.com

Éder Lima de Albuquerque

eder@unb.br

Universidade de Brasília, Faculdade de Tecnologia, Departamento de Engenharia Mecânica, Distrito Federal, 70910900, Brasil

Luís Wrobel

luiz.wrobel@brunel.ac.uk

Brunel University London, Institute of Materials and Manufacturing, Department of Mechanical, Aerospace and Civil Engineering.

Abstract. This paper presents an adaptive cross approximation (ACA) accelerated Isogeometric Boundary Element Method (IBEM) using Non-Uniform Rational B-Splines (NURBS) as shape and interpolation functions. Provided that NURBS are used in CAD programs to describe geometry, the mesh generation in the IBEM is no longer necessary. For large and complex models the traditional BEM quickly becomes very time and memory consuming and, to overcome this problem, the use of ACA is considered in this paper. Mesh generation is also found to be one of the most time consuming tasks in numerical simulations, therefore the coupling between ACA and IBEM is very promising. Numerical examples are presented in order to assess the accuracy and feasibility of the method.

Keywords: Boundary Element Method, Isogeometric analysis, ACA.

1   Introduction

Discretization procedures used in engineering problems lack the continuity of derivatives of variables between adjacent elements. This behaviour is expected due to the piecewise characteristics of its shape functions and generally introduces an inaccuracy. This problem is found both in the Finite Element Method (FEM) and the Boundary Element Method (BEM), but it is particularly relevant for the BEM because the problem solution is fully described in terms of the boundary variables [2].

The most popular schemes for preserving derivative continuity use splines and several types can be found in the literature: standard, Overhauser, Bezier, B-splines, Non Uniform Rational Basis Splines (NURBS), T-splines and PHT-splines. These entities are commonly found in Graphical Design. Different types of splines have already been used on BEM but the usage of NURBS is quite recent ([10] and [9]). Using the same basis functions to approximate both the field variables and the geometry generates a method that does not require creating a mesh since the same discretization used by the geometry will used in the boundary element analysis, thus creating an isogeometric method.

This type of integration between CAD and the analysis method was first presented in [6]. This paper will present an isogeometric formulation accelerated by ACA for two-dimensional potential problems.

2   NURBS

A NURBS curve is defined by its order, a set of weighted control points, and a knot vector. NURBS curves and surfaces are generalizations of both B-splines and Bezier curves and surfaces. The primary difference being the weighting of the control points which makes NURBS curves rational (non-rational B-splines are a special case of rational B-splines).

The shape of the curve is determined by control points. Each point of the curve is computed by taking a weighted sum of a number of control points multiplied by basis functions. For a curve of degree d, the basis function of any control point is only nonzero in $d + 1$ intervals of the parameter space. Within those intervals, the basis functions change according to a rational polynomial function. At boundaries of intervals, basis functions go smoothly to zero, the smoothness being determined by the degree of the polynomial.

The knot vector is a sequence of parameter values that determines where and how control points affect the NURBS curve. The number of knots is equal to the number of control points plus the order of the curve. The knot vector divides the parametric space in intervals, referred to as knot spans. Each time the parameter value enters a new knot span, a new control point becomes active, while an old control point is discarded.

Consecutive knots can have the same value. This defines a knot span of zero length, which implies that two control points are activated at the same time (and consequently two control points become deactivated). This alters the continuity of the curve allowing the creation of corners in an otherwise smooth NURBS curve. A number of coinciding knots is known as a knot with a certain multiplicity. The multiplicity of a knot is limited to the degree of the curve, since a higher multiplicity would split the curve into disjoint parts and it would leave control points unused.

The B-spline basis functions used in the construction of NURBS curves is denoted as $N_{i,k}(u)$, in which i corresponds to the i-th control point, and k corresponds to the degree of the basis function. The function is computed as

$$N_{i,k}(u) = \frac{u - t_i}{t_i + k - t_i} N_{i,k-1}(u) + \frac{t_{i+k+1} - u}{t_{i+k+1} - t_{i+1}} N_{i+1,k-1}(u) \tag{1}$$

and

$$N_{i,0}(u) = \begin{cases} 1, \text{if } t_i <= u < t_{i+1} \\ 0, \text{otherwise} \end{cases} \tag{2}$$

The definition of these basis functions is clearly recursive.

Once these functions are defined one can calculate the piecewise rational polynomial function that is the NURBS basis function:

$$C(u) = \sum_{i=0}^{n} \frac{w_i \times P_i \times N_{i,k}(u)}{w_i \times N_{i,k}(u)}. \tag{3}$$

A NURBS surface representation is a straightforward extension of a NURBS curve. By doing a tensor product between two sets of basis functions one can obtain the surface $S(u, v)$ as:

$$S(u, v) = \frac{\sum_{i=0}^{n} \sum_{j=0}^{m} N_{i,p}(u) N_{j,q}(v) w_{i,j} P_{i,j}}{\sum_{i=0}^{n} \sum_{j=0}^{m} N_{i,p}(u) N_{j,q}(v) w_{i,j}}. \tag{4}$$

It is worthwhile to use a rational basis definition, such as:

$$R_{i,j}(u, v) = \frac{N_{i,p}(u) N_{j,q}(v) w_{i,j}}{\sum_{k=0}^{n} \sum_{l=0}^{m} N_{k,p}(u) N_{l,q}(v) w_{k,l}}. \tag{5}$$

With this definition, the surface equation can be simplified to:

$$S(u, v) = \sum_{i=0}^{n} \sum_{j=0}^{m} R_{i,j}(u, v) P_{i,j}. \tag{6}$$

Equation (6) is the one that will be used in isogeometric analysis, it relates the values at the control points to values in the surface.

3   Boundary element method

The isogeometric boundary element method differs from the conventional BEM on three main points:

- The basis functions for the geometry and field variables,

- The position of the collocation points,

- The application of the boundary conditions.

A direct collocation form of the BEM consists in constructing a system of equations by taking a collocation point for every unknown and applying to a boundary integral equation. For potential problems, the integral equation that relates the potential and its derivative is given as:

$$cu(P) = \int_s \frac{\partial u}{\partial n} u^* ds - \int_s u \frac{\partial u^*}{\partial n} ds \qquad (7)$$

where c is a jump term that arises from the limiting process of the integral equation and is dependent on the geometry at the source point, u and $\frac{\partial u}{\partial n}$ are the potential and its derivative in the normal to the boundary direction, respectively, while u^* and $\frac{\partial u^*}{\partial n}$ refers to the fundamental solutions.

In order to make equation (7) suitable for numerical implementation, the continuous fields u and $\frac{\partial u^*}{\partial n}$ have to be represented in a discrete manner. In the conventional BEM, the idea is to split the boundary in elements that use a Lagrange interpolation while in the isogeometric method the geometry is exactly obtained from the CAD model and the basis functions from equations (3) and (6) are used to approximate the variables. This leads to:

$$cu(x) = \int_\Gamma \sum_{i=1}^{n+1} (u_i^c R_{i,k}(t)) \frac{\partial u}{\partial n} u^*(x,x') ds - \int_\Gamma u^*(x,x') \sum_{i=1}^{n+1} \left(\frac{\partial u_i^c}{\partial n} R_{i,k}(t) \right) ds. \qquad (8)$$

The boundary integrals in conventional BEM can be easily divided in elements whereas in isogeometric the definition of elements is not obvious. A easy way to define is separating the knot spans in domains of influence of each control point, resulting in:

$$cu(x) = \sum_{i=1}^{n+1} \left(u_i^c \int_{t_i}^{t_{i+k}} R_{i,k}(t) \frac{\partial u^*}{\partial n}(x,x') \frac{d\Gamma}{dt} dt \right) - \sum_{i=1}^{n+1} \left(\frac{\partial u_i^c}{\partial n} \int_{t_i}^{t_{i+k}} u^*(x,x') R_{i,k}(t) \frac{d\Gamma}{dt} dt \right)$$

$$\qquad (9)$$

where, finally, one can do a transformation to a standard domain in order to easily integrate numerically using Gauss-Legendre quadrature:

$$\sum_{i=1}^{n+1} \left(u_i^c \left(\int_{-1}^{1} R_{i,k}(t) \frac{\partial u^*}{\partial n}(x,x') \frac{d\Gamma}{dt} \frac{dt}{d\xi} d\xi - cR_{i,k}(x') \right) \right) =$$

$$\sum_{i=1}^{n+1} \left(\frac{\partial u_i^c}{\partial n} \int_{-1}^{1} u^*(x,x') R_{i,k}(t) \frac{d\Gamma}{dt} \frac{dt}{d\xi} d\xi \right). \qquad (10)$$

The jacobian of the transformation comprises of two terms: one that maps from the physical coordinate space, $\frac{d\Gamma}{dt}$ and one that maps from the parameter space of the curve to a local coordinate $\frac{dt}{d\xi}$.

The same straightforward procedure can be applied to potential and elastic in both two and three dimensions. For three dimensions, the resulting equation is given as:

$$\sum_{i=1}^{n+1} \left(u_i^c \left(\int_{-1}^{1} \int_{-1}^{1} R_{i,k}(t) \frac{\partial u^*}{\partial n}(x, x') J \frac{du}{d\xi} \frac{dv}{d\eta} d\xi d\eta - cR_{i,k}(x') \right) \right) =$$
$$\sum_{i=1}^{n+1} \left(\frac{\partial u_i^c}{\partial n} \int_{-1}^{1} \int_{-1}^{1} u^*(x, x') R_{i,k}(t) J \frac{du}{d\xi} \frac{dv}{d\eta} d\xi d\eta \right), \quad (11)$$

where the surface integrals are transformed into double integrals in a standard domain.

3.1 Integration

The evaluation of boundary integrals is key to any BEM implementation. However, in isogeometric BEM, a special care is needed since the strongly singular integrals cannot be obtained indirectly through constant temperature or rigid body motion hypothesis. The values at the collocation points are not interpolated as in the conventional BEM. They are approximated, resulting in multiples singular integrals for each equation. The method of choice for dealing with strongly singular integrals is the singularity subtraction technique presented by [4] for two dimensional problems and by [12] for three dimensional problems. Weakly singular integrals are calculated using the Telles [11] transformation in two dimensions, while in three dimensions the singular area integral is dealt with by transforming it into polar coordinates.

The choice for collocation points used in this work makes it simple to obtain the jump term c since their position will always be on a smooth boundary, resulting in a c always equal to $1/2$.

3.2 Collocation points

The control points and the knots used to define NURBS are not required to be unique, as mentioned earlier; they can have a multiplicity up to the degree of the curve. The control points are not located at the boundary but on a circumscribed polygon. These characteristics make these entities not the best choices for collocation points on the BEM. The domain point over which a control point has maximal influence is called a Greville abscissa [3] and is defined as an average of d knots :

$$\gamma_i = \frac{1}{d}(t_{i+1} + ... + t_{i+d}). \tag{12}$$

These points are unique, located at the boundary and are equal in number to the control points. When the curve is smooth, these are the ideal candidates to be used as collocation points, and are used in such manner in [10] and [9]. However, when corners are present, specially for 3D problems, it becomes troublesome to calculate the diagonal terms since the collocation points are at the corners.

To circumvent this issue, collocation points are, in this work, distributed according to the points of the Gaussian quadrature:

$$\gamma_i = \frac{(t_{i+1} - t_{i+2})(\xi + 1)}{2} + t_{i+1} \tag{13}$$

where ξ is the coordinate of the Gauss points. If all knots are unique, the number of knot spans, with length different from zero, is equal to the number of control points and only one Gauss point is used. Therefore, the collocation points will be at the center of each knot span. When the knot has a multiplicity larger than one the number of Gauss points is increased, maintaining an equal number of collocation points and control points.

Considering that the Gauss points are never at the limits of the integration interval, collocation points will also never be at a corner of the curve.

This procedure resembles the use of discontinuous elements but no change in the control points is made and consequently there is no loss of continuity in the approximation.

4   Adaptive cross approximation

The ACA acceleration process starts by dividing the geometric domain in a tree data structure. This division creates, in each tree node, a cluster of collocation points or control points that are close to each other. When the distance between a pair of collocation and control points is large enough, the block defined from those entries is considered admissible and is represented by a low rank approximation. The remaining blocks are generated in the usual BEM manner and are stored as full matrices. A thorough presentation of ACA can be found in [1] and [7].

The savings in memory and time are due to the low rank approximations. This format needs less entries than a full matrix and is much faster when multiplying a vector. Most iterative methods for solving linear systems are based on matrix-vector multiplication and if that is optimised, the whole method will become more efficient.

The procedure involved in calculating the low rank approximations in ACA has to evaluate exactly a column and a row at a time. For constant elements, this can be done easily as each column is related to a specific element and therefore also a specific node. When dealing with isogeometric BEM, there is no proper definition of element and each control point has a unique, but intersecting, interval in which its basis function is non-zero.

That interval can be understood as the domain of influence of each control point and is defined as:

$$Domain_i = (t_{i+1}, t_{i+d}) \tag{14}$$

To calculate a single column, there is only the need to integrate the domain of influence of the corresponding control point. By working in such manner, the basis function and geometric properties of the Gauss points will only be calculated once for each column. It is important reminding that the evaluation of NURBS basis functions is much more expensive than for regular polynomial basis functions. When calculating a row, it is necessary to integrate over all the

domains of influence of the corresponding control point. By definition, when one seeks a low rank approximation, the field and source points are relatively far from each other, therefore one can expect that fundamental solutions will change smoothly leading to the possibility of using a very low number of Gauss points, half the order of the curve plus one for example, and still obtaining a satisfactory approximation.

5   Boundary conditions

As control points are typically outside the boundary, boundary conditions cannot be applied directly. In order to overcome this issue a transformation matrix $\mathbf{E}$ for B-splines was proposed in [2]. This matrix uses the basis functions to relate the values at the control points with the values at the collocation points:

$$\mathbf{u} = \mathbf{E}\mathbf{u}_c \tag{15}$$

$$\frac{\partial \mathbf{u}}{\partial \mathbf{n}} = \mathbf{E}\frac{\partial \mathbf{u_c}}{\partial \mathbf{n}} \tag{16}$$

where $\mathbf{u}$ is a vector containing the values at the collocation points and $\mathbf{u}_c$ is the vector containing values at the control points. An equivalent matrix can be obtained for NURBS using the equilibrium equation derived in [2]:

$$\mathbf{H}\mathbf{u}_c = \mathbf{G}\frac{\partial \mathbf{u_c}}{\partial \mathbf{n}} \tag{17}$$

which is rewritten as:

$$\mathbf{H}\mathbf{E}^{-1}\mathbf{u} = \mathbf{G}\mathbf{E}^{-1}\frac{\partial \mathbf{u}}{\partial \mathbf{n}}. \tag{18}$$

This procedure becomes an issue when one tries to use ACA. The inverse of the transformation matrix is not sparse and the method would become unable to be accelerated by ACA, as the Hierarchical matrices $\mathbf{H}$ and $\mathbf{G}$ would turn into full matrices after being multiplied by $\mathbf{E}^{-1}$.

What is proposed is that we add a knot with maximum multiplicity for every change in boundary condition type. By doing so, intervals with different boundary conditions can be separated and values at control points can be found by solving a simple linear system for each interval:

$$\mathbf{u}_c = \begin{bmatrix} \mathbf{E}_0^{-1}\mathbf{u}_0 \cdots \mathbf{E}_i^{-1}\mathbf{u}_i \cdots \mathbf{E}_n^{-1}\mathbf{u}_n \end{bmatrix} \tag{19}$$

$$\frac{\partial \mathbf{u_c}}{\partial \mathbf{n}} = \begin{bmatrix} \mathbf{E}_0^{-1}\frac{\partial \mathbf{u_0}}{\partial \mathbf{n}} \cdots \mathbf{E}_i^{-1}\frac{\partial \mathbf{u_i}}{\partial \mathbf{n}} \cdots \mathbf{E}_n^{-1}\frac{\partial \mathbf{u_n}}{\partial \mathbf{n}} \end{bmatrix}. \tag{20}$$

This procedure does not change the geometry but the points where boundary condition changes become only C_0 continuous. For most cases, that should not be an issue.

6   RESULTS

In this session, in order to assess the potential isogeometric formulation, two two-dimensional and 4 three-dimensional problems will be analysed. Results will be compared with constant elements and the analytical response. For the 3D problems, results for the conventional BEM are obtained with the software provided by [8], that uses constant triangular elements and the fast multipole method. The normalized root mean square error is used as a error measure in some instances. This estimator is given by:

$$e_{rms} = \frac{\sqrt{\frac{\sum_{t=1}^{n}(y_t - y_a)^2}{n}}}{y_{max} - y_{min}}. \tag{21}$$

where y_t is the numerically obtained value at point t, y_a is the analytical value, n is the number of points, y_{max} and y_{min} are the maximum and minimum values of variable y_a.

6.1   Heat transfer in a cylinder

The first problem is the heat transfer on a cylinder that will be modelled in 2D as shown in figure 1. This problem has analytical solution and will be used to assess results. The temperature is known at the internal boundary S_i and the flux is known at the external boundary S_e. The analytical solution for the temperature is given by:

$$T(r) = T_i + q_e r_e \log\left(\frac{r}{r_i}\right) \tag{22}$$

and for the flux:

$$q(r) = q_e \frac{r_e}{r} \tag{23}$$

where T_i e q_e are the temperature and flux at the internal and external boundary, respectively.
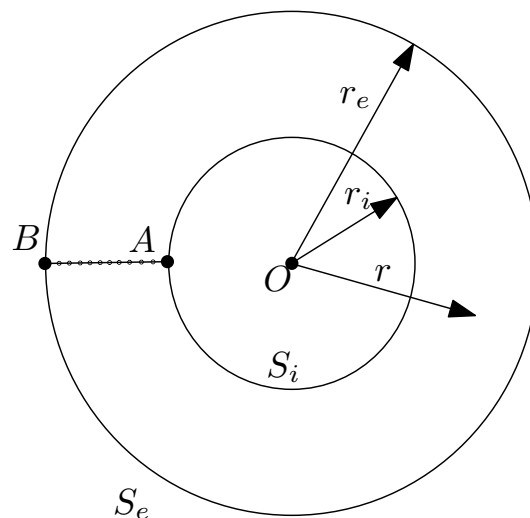

Figure 1: Potential problem in an annular region.

For this problem the following values are considered: $r_i = 1$, $r_e = 2$, $T_i = 100$, $q_e = 200$ and $k = 1$. This results in a analytical response of $T_e = 377,258872$ and $q_i = -400$. The external and internal boundary are discretized with the same number of elements. In figures 2 and 3, relative errors for the temperature at point B and flux at point A are shown for constant and isogeometric elements.
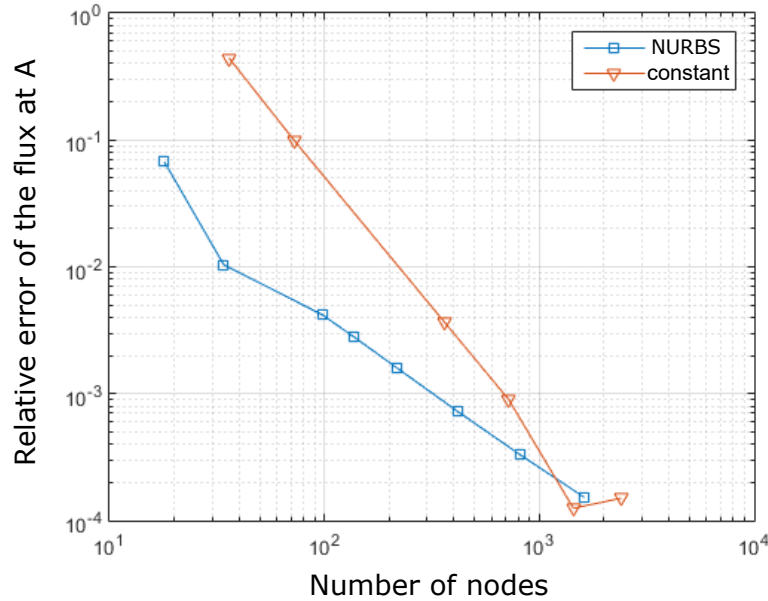

Figure 2: Flux errors at A**.**

Both the conventional method and the isogeometric method converge to the exact solution. The isogeometric discretization has a better response with few elements while constant elements have a faster convergence. As all variables are constant, the biggest difference between the methods is the geometry representation. Even the poorest discretization represents the geometry exactly for the isogeometric method.

The RMS errors is used to show the approximation at internal points. The temperature is calculated at 10 uniformly distributed points along segment AB. The RMS error and the maximum error are calculated and shown in figure 4.

The error obtained by the isogemetric method is smaller than the constant even for a number of nodes where the error at the boundary for the conventional method is smaller. This is explained by the exact representation of the boundary in the isogeometric method. As the representation is better it will lead to smaller errors in the boundary integral.

6.2 Rectangular plate

The problem analysed is a rectangular plate as shown in figure 5.

Where the boundary conditions are:

$$q = -\frac{1}{2\sqrt{r}}\left(\cos\frac{\theta}{2}\cos\theta + \sin\frac{\theta}{2}\sin\theta\right) \text{ in } BC, \tag{24}$$
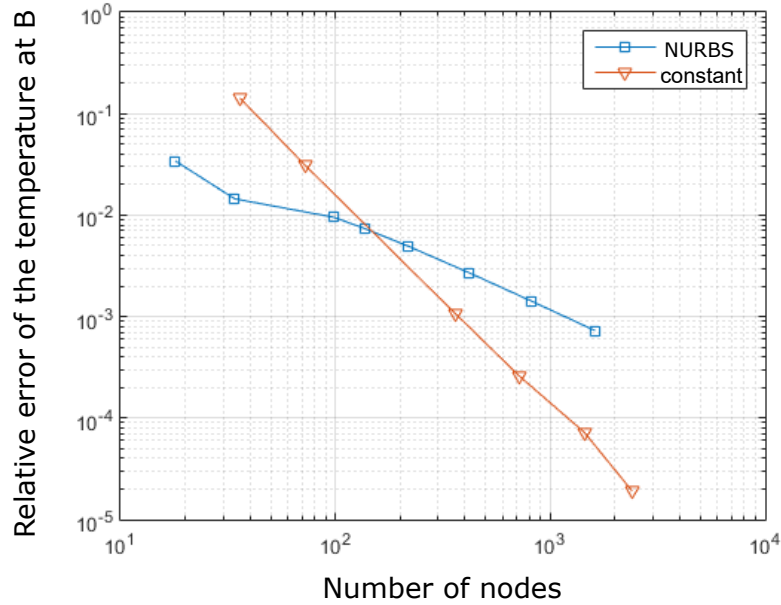
Figure 3: Temperature errors at B.

$$q = -\frac{1}{2\sqrt{r}} \left(\cos\frac{\theta}{2} \cos\theta - \sin\frac{\theta}{2} \sin\theta \right) \text{ in } CD, \tag{25}$$

$$q = \frac{1}{2\sqrt{r}} \left(\cos\frac{\theta}{2} \cos\theta + \sin\frac{\theta}{2} \sin\theta \right) \text{ in } DA, \tag{26}$$

$$T = 0 \text{ in } AO \tag{27}$$

and

$$q = 0 \text{ in } OB. \tag{28}$$

This problem has an analytical solution and it is given by:

$$u = \sqrt{r} \cos\frac{\theta}{2}; \tag{29}$$

$$q_x = \frac{\cos\frac{\theta}{2}}{2\sqrt{r}} \tag{30}$$

and

$$q_y = \frac{\sin\frac{\theta}{2}}{2\sqrt{r}}. \tag{31}$$

Figures 6 and 7 show the relative error of temperature at point E for isogeometric elements of various orders and constant elements. In figure 6, the proposed method for imposing the boundary conditions is utilized, while at figure 7 no special care is taken. There is a clear difference: results obtained with the proposed method are superior to the alternative. This a good problem to show the efficiency of the method as the imposed boundary conditions are not
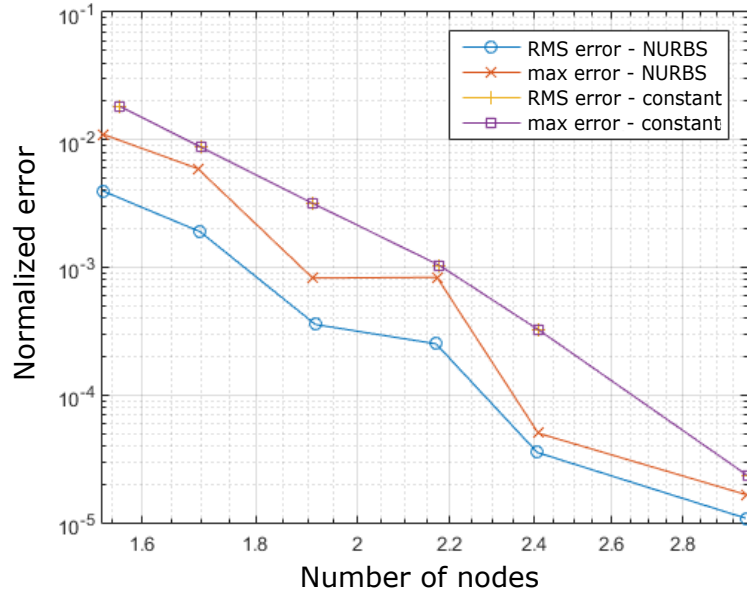
CILAMCE 2016

Proceedings of the *XXXVII Iberian Latin-American Congress on Computational Methods in Engineering*
Suzana Moreira Ávila (Editor), ABMEC, Brasília, DF, Brazil, November 6-9, 2016
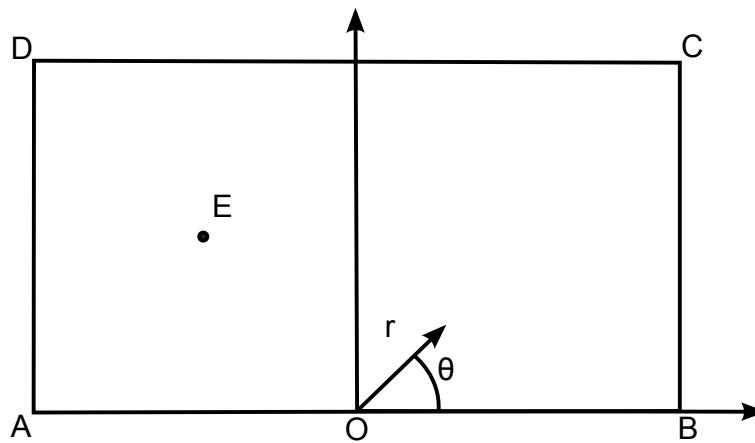
Figure 4: Temperature errors along AB.

Figure 5: Rectangular plate.

constant. They are, in fact, quite complex, there is even a singularity at point O. While even the conventional method represents the geometry exactly, as it is quite simple.

Results at figure 6 show a improvement as the order increases. However, even for the element with the lowest order, 2, there is an improvement when compared to the conventional method.

6.3 Sphere

The example shown in [13] will be analysed here. The problem consists in spherical structure of radius equal to 1 and centre $(0.5, 0.5, 0.5)$ as shown in figure 8. The temperature prescribed at the boundary is:
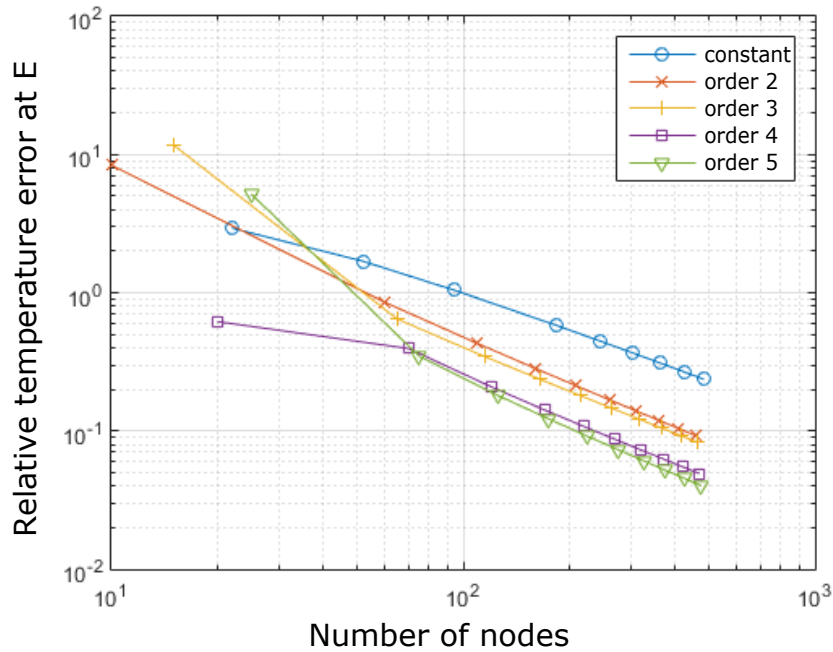
$$u = x^2 - y^2 + 2x + z \tag{32}$$

Figure 6: Errors at point E for the proposed method.

Table 1: Normalized RMS error for the sphere.

Constant elements		Order 3 isogeometric elements	
Nodes	Normalized RMS Errors	Nodes	Normalized RMS Errors
320	0.017847	45	0.0110208
1280	0.011417	91	0.00231124
5120	0.010104	153	0.00151761
20480	0.0099437		

the analytical solution for the flux is given by $-k\mathbf{n}\nabla u$ where:

$$\nabla u = [2x + 2 \quad -2y \quad 1].$$
(33)

At table 1, the normalized RMS errors is shown for both isogeometric elements of order 3 and triangular constant elements. In this comparison, it becomes clear that the performance of isogeometric elements is superior to regular elements. However, the NURBS representation of the sphere generates two poles that concentrate the control points, as seen in figure 8. This concentration requires a special attention in dealing with the singularities. The treatment of the singular integrals suffer with element distortion [5] requiring over 500 integrations points, when near the poles, in order to obtain an error smaller than 10^{-6}.
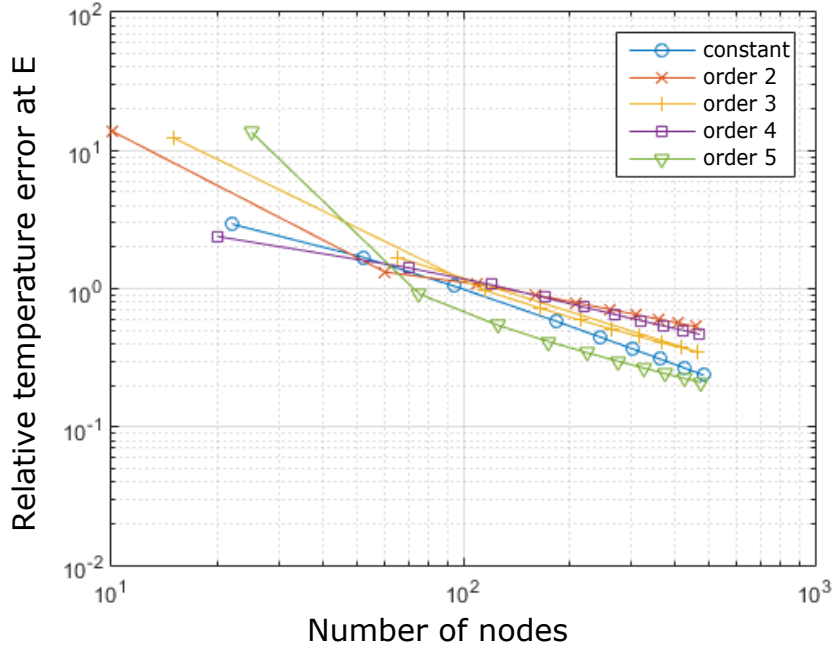
Figure 7: Errors at point E without the proposed method.

6.4 Torus

This example, presented by [13], a torus of external radius and internal radius equal to $R = 2$ e $r = 1$, respectively, is analysed with a temperature at the boundary equal to:

$$u = \frac{x^2}{2} + \frac{y^2}{2} - z^2 + 5x + 5y + 5z \tag{34}$$

and the analytical solution of the flux is given by $-k\mathbf{n}\nabla u$, where:

$$\nabla u = [x + 5 \quad y + 5 \quad -2z + 5]. \tag{35}$$

At figure 9 the flux obtained with 81 control points is shown. There is no concentration of control points in this geometry, that leads to a less troublesome singularity treatment when compared to the sphere.

At table 2, where the RMS errors for the collocation points are shown, a clear advantage of the isogeometric method, when compared to the constant element can be observed. In [13] a comparison can be made with the quadratic elements, where, even with the use of 1600 elements, the error is still higher than 10^{-3}.

6.5 Square plate with holes

In order to test the efficiency of ACA in the execution time of the method, a square plate with a growing number of uniformly distributed holes is analysed. At figure 10, one can observe
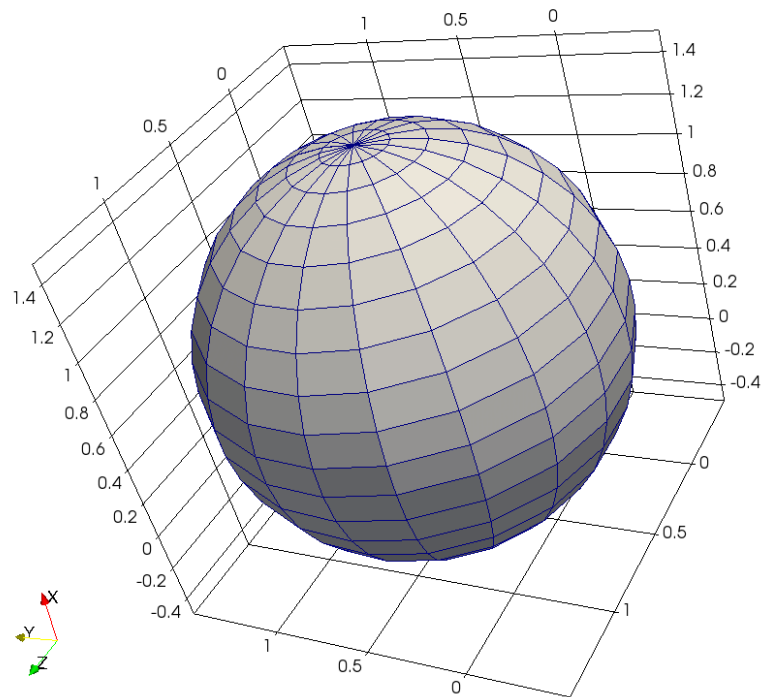
Figure 8: Sphere represented with NURBS.
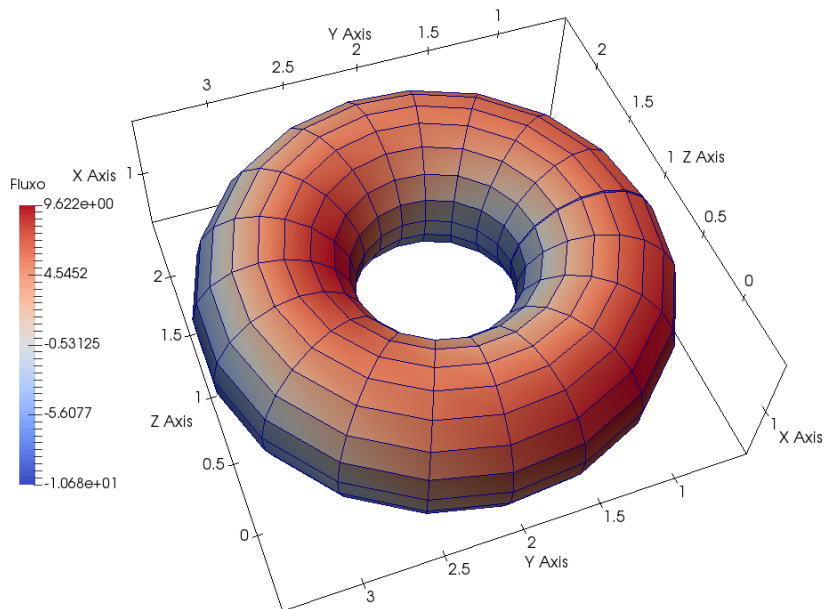

Figure 9: Torus represented by NURBS.

CILAMCE 2016

Proceedings of the *XXXVII Iberian Latin-American Congress on Computational Methods in Engineering*
Suzana Moreira Ávila (Editor), ABMEC, Brasília, DF, Brazil, November 6-9, 2016

Table 2: Normalized error for the torus

Constant elements		Order 3 isogeometric elements	
Nodes	Erro RMS normalizado	Nodes	Erro RMS normalizado
1792	0.0086708	81	0.0176615
28224	0.0098135	169	0.0027632
		441	0.000568215

$T = 1$ $T = 0$

Figure 10: Plate with holes.

CILAMCE 2016

Proceedings of the XXXVII Iberian Latin-American Congress on Computational Methods in Engineering
Suzana Moreira Ávila (Editor), ABMEC, Brasília, DF, Brazil, November 6-9, 2016

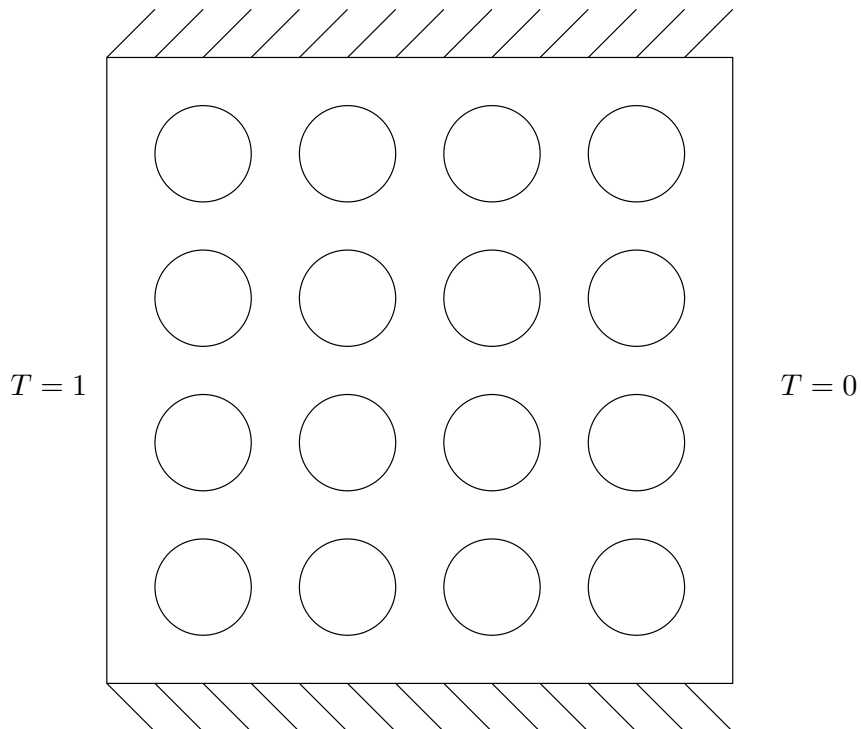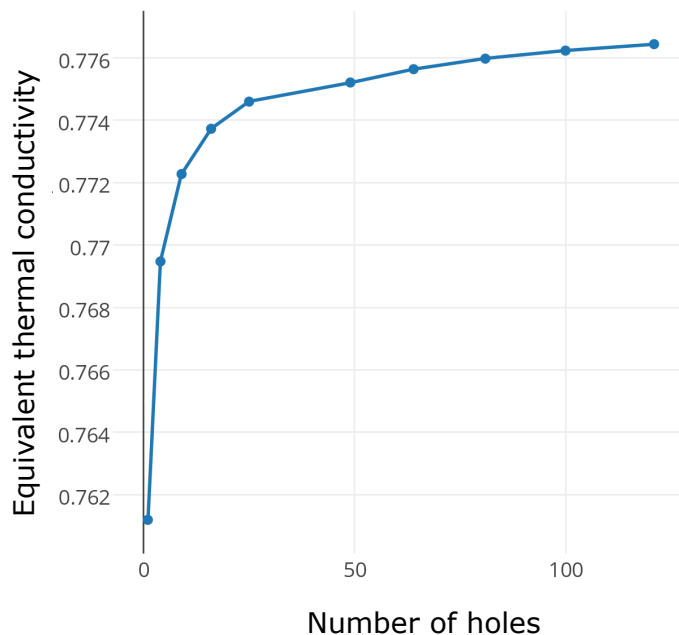**Figure 11: Thermal conductivity for different quantities of holes.**

the case for 16 holes. The size of the holes is modified in such a way that the ratio between the area of the holes and the area of the plate remains constant and equal to 12,47%.

An equivalent thermal conductivity can be calculated by dividing the flux at one of the sides of the plate by the flux at the plate without holes. The value of the equivalent conductivity, for different quantities of holes, is shown at figure 11. It can be observed, that the conductivity converges as the quantity of holes increases.

The execution time as the number of holes increases, from 1 until 121, is shown in figure 12. The change of slope of the curves shows the evident improvement in speed: the standard method has a slope close to n^2 while the one using ACA is close to $n \log n$. Even though the accelerated method is slower for small problems, the different in slope make it faster for larger problems.

7 CONCLUSION

This work presented a proper way to couple NURBS and ACA, taking special care with the boundary conditions, resulting in a method that is very interesting for large and complex CAD models. The usage of ACA provides memory saving and running time reduction when compared to regular BEM. In isogeometric formulation, as it uses the CAD parameters directly, there is no need to created a mesh. This drastically reduces the engineering work in the numerical analysis.
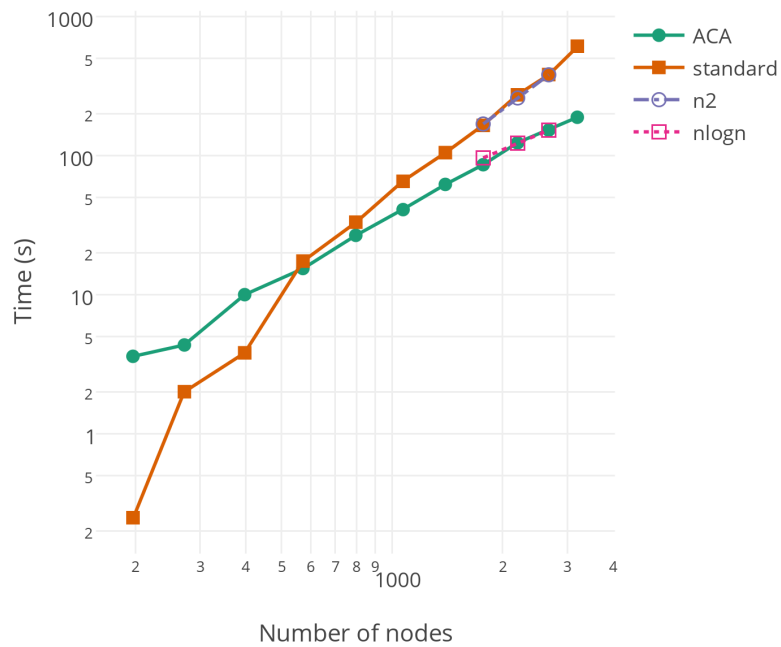
Figure 12: Execution time for various holes.

The position of collocation points makes it formulation easier to implement, specially for 3D, since there are no collocation points at corners. As the curve is always smooth, there is no need for a special treatment for the diagonal terms. However, quasi-singularities are present, since the points are near the corner. When there is a concentration of the control points, as in the sphere, the integral became even more troublesome.

The method for imposing the boundary conditions is shown to be precise while maintaining the beneficial properties of the hierarchical matrices. The order of complexity of the method goes from n^2 to $n \log n$ by taking advantage of the ACA. The proposed method is not only faster and more memory efficient but also more precise than the standard method.

CILAMCE 2016

Proceedings of the *XXXVII Iberian Latin-American Congress on Computational Methods in Engineering*
Suzana Moreira Ávila (Editor), ABMEC, Brasília, DF, Brazil, November 6-9, 2016

Bibliography

[1] Mario Bebendorf. *Hierarchical matrices: a means to efficiently solve elliptic boundary value problems*, volume 63. Springer, 2008.

[2] JJSP Cabral, LC Wrobel, and CA Brebbia. A bem formulation using b-splines: I-uniform blending functions. *Engineering analysis with boundary elements*, 7(3):136–144, 1990.

[3] Gerald E Farin. *Curves and Surfaces for Computer-Aided Geometric Design: A Practical Code*. Academic Press, Inc., 1996.

[4] MASSIMO Guiggiani, GUNA Krishnasamy, TJ Rudolphi, and FJ Rizzo. A general algorithm for the numerical solution of hypersingular boundary integral equations. *Journal of applied mechanics*, 59(3):604–614, 1992.

[5] K Hayami and H Matsumoto. Improvement of quadrature for nearly singular integrals in 3d-bem. *WIT Transactions on Modelling and Simulation*, 7, 1994.

[6] Thomas JR Hughes, John A Cottrell, and Yuri Bazilevs. Isogeometric analysis: Cad, finite elements, nurbs, exact geometry and mesh refinement. *Computer methods in applied mechanics and engineering*, 194(39):4135–4195, 2005.

[7] Stefan Kurz, Oliver Rain, and Sergej Rjasanow. Fast boundary element methods in computational electromagnetism. In *Boundary Element Analysis*, pages 249–279. Springer, 2007.

[8] Yijun Liu. *Fast multipole boundary element method: theory and applications in engineering*. Cambridge university press, 2009.

[9] MA Scott, Robert Napier Simpson, JA Evans, S Lipton, Stephane Pierre Alain Bordas, TJR Hughes, and TW Sederberg. Isogeometric boundary element analysis using unstructured t-splines. *Computer Methods in Applied Mechanics and Engineering*, 254:197–221, 2013.

[10] Robert Napier Simpson, Stephane Pierre Alain Bordas, J Trevelyan, and T Rabczuk. A two-dimensional isogeometric boundary element method for elastostatic analysis. *Computer Methods in Applied Mechanics and Engineering*, 209:87–100, 2012.

[11] J. C. F. Telles. A self-adaptive co-ordinate transformation for efficient numerical evaluation of general boundary element integrals. *International Journal for Numerical Methods in Engineering*, 24(5):959–973, 1987.

[12] C. J. B. Ubessi. Método dos elementos de contorno para elasticidade linear 3d com avaliação direta das integrais singulares. *Dissertação - UFRGS*, 2014.

[13] Yaoming Zhang, Yanpeng Gong, and Xiaowei Gao. Calculation of 2d nearly singular integrals over high-order geometry elements using the sinh transformation. *Engineering Analysis with Boundary Elements*, 60:144–153, 2015.

CILAMCE 2016

Proceedings of the XXXVII Iberian Latin-American Congress on Computational Methods in Engineering
Suzana Moreira Ávila (Editor), ABMEC, Brasília, DF, Brazil, November 6-9, 2016